Multichannel predictive deconvolution and Parabolic Radon Transform for multiple reflection's filtering on land seismic data from Solimoes basin

Misael Possidonio de Souza,* and Milton J. Porsani. CPGG/UFBA, and Michelângelo Gomes da Silva CPGG/UFBA

Abstract

The Solimoes basin became the target of oil exploration campaigns after the discovery of the Juruá field in the 1970s. Its geological evolution is marked by magmatic spills represented by the diabase sills, which, in addition to preventing seismic energy, generate Multiple reflections, creating problems in processing. This work proposes the application of multichannel predictive deconvolution and Parabolic Radon Transform for the attenuation of multiple reflections. The results showed that although the periodicity of these events was not perfect, both methods were effective in land seismic data, attenuating multiple reflections and preserving primary reflections.

Introduction

Despite the current unfavorable scenario for oil research, which leads large companies to focus only marine sedimentary basins and pre-salt, exploration of oil in new basins such as the Solimoes basin will still be the subject of many discussions in the future, given the success of exploration in the 1970s, with the discovery of commercial gas field. The geology of this basin is characterized by significant volumes of magma during the rift phase, which are the diabase sills, present in almost every area of its geology, the sills are easily seen in a stacked section as reflectors of strong amplitude associated to its tops and bases. It has a depocentro in the range of 3300 meters and an area of approximately 950 thousand square kilometers. This basin underwent a tectonic event during the Mesozoic, Juruá Tectonic, generating folds, reverse faults and anticlines, being the main structures of the petroleum system of this basin. The diabase sills act as a kind of barrier to seismic energy, making it difficult to propagates the layers underneath the sills. In addition, these magmatic spills create internal multiple and surface reflections, as well as many reverberations, making the seismic data processing even more difficult. The analyzed data were acquired using the split-spread acquisition geometry, with distance between shots of 50m and distance between receivers of 25m. Conventional seissmic processing flow was followed using the Seisspace/ProMax 2D for Parabolic radon filtering and Seismic Unix package for deconvolution implementation available in the CPGG / UFBA.

Methodology

Predictive Multichannel deconvolution

The following is the procedure for obtaining multichannel WL filters using 3 channels and number of filter coefficients per channel equal to 3. Let w, the desired data, x, y and z, the three strokes Then the calculated data w, can be represented by the expression,

$$\tilde{w} = \tilde{h}(t) * x(t) + \tilde{f}(t) * y(t) + \tilde{g}(t) * z(t), \quad (1)$$

Where $h(t)$, $f(t)$, $g(t)$ are operators acting respectively on the traits x, y and and z. Exemplifying for operators with three coefficients in each signal, the above expression can be rewritten,

$$\tilde{w}_t = \sum_{k=1}^{3} x_{t-k+1}\tilde{h}_k + \sum_{k=1}^{3} y_{t-k+1}\tilde{f}_k + \sum_{k=1}^{3} z_{t-k+1}\tilde{g}_k \quad (2)$$

using matrix notation we can write,

$$\mathbf{W} = [\mathbf{X} \quad \mathbf{Y} \quad \mathbf{Z}] \quad (3)$$

$\mathbf{W}$ is a toeplitz matrix constructed by the matrices, also toeplitz, $\mathbf{X}$, $\mathbf{Y}$ and $\mathbf{Z}$ respectively generated by the traces x_t, y_t and z_t and $\mathbf{a}$ is a vector formed by the vectors $\mathbf{h}$, $\mathbf{f}$ and $\mathbf{g}$. We can then define $\mathbf{a^T}$ by:

$$\mathbf{a^T} = [\mathbf{h^T} \quad \mathbf{f^T} \quad \mathbf{g^T}] \quad (4)$$

where the vectors $\mathbf{h}$, $\mathbf{f}$ e $\mathbf{g}$ are formed by the operators $\tilde{h}_t$, $\tilde{f}_t$ e $\tilde{g}_t$. For a random vector $\mathbf{a}$, we can relate the predicted error vector by:

$$\mathbf{e} = \mathbf{x} - \mathbf{W}\mathbf{a} \quad (5)$$

minimizing the quadratic error we find:

$$Q(\mathbf{a}) = \mathbf{e^T} - \mathbf{e} \quad (6)$$

and obtaining the Normal Equations, whose solution provides WL multi-channel predictive filter.

The Parabolic Radon Transform

The Parabolic Radon Transform maps parabolic events with different apertures where the amplitudes are summed along these parabolas , resulting in points or regions of coherence in the $\tau - q$ domain, with the different parabolas being concentrated in different regions. Basically, we change the data domain to separate multiple reflections against primary refletcions by the move-out difference.

Hampson introduced the radon parabolic transform and all its mathematical formulation, as well as its applications

in seismic data. Basically the data are organized into common midpoint families or CMPs families, and the NMO correction is done through the equation:

$$t = \sqrt{t^2 - \frac{4x^2}{v^2}}, \tag{7}$$

where t after the NMO correction and v is the speed used in the NMO correction and x, the offset. An approximation of the travel time in the parabolic form is expressed in the equation below as:

$$t = \tau + qx^2 \tag{8}$$

where tau represents the travel time of the wave for the zero-offset case and q, the curvature of this parabola. Thus, the direct Radon transform results in the sum of the amplitudes along the parabola in the CMP domain, given by:

$$v(q,\tau) = Ru(q,\tau) = \sum_x u(x, t = \tau + qx^2), \tag{9}$$

with $v(q,\tau)$ as a sum along the parabola. In the $tau - p$ domain, the primary reflections will be separated from the multiple reflectios. However the inverse Radon transform is not fully reversible, witch is a problem related to the discretization of the data and various limitations associated with the acquisition. Therefore, an inverse transform estimate based on least squares methods is used. Thus, the inverse Radon transform, in the expression:

$$u^{'}(x,t) = R * v(q,\tau) = \sum_q v(q, \tau = t - qx^2), \tag{10}$$

and its matrix form:

$$\mathbf{u'} = \mathbf{Lv}, \tag{11}$$

where L is the operator that takes the seismic information from the $\tau - q$ domain to the CMP domain. The error e between the registered data u and the CMP domain data through the inverse transform, $u^{'}$ is given by:

$$\mathbf{e} = \mathbf{u} - \mathbf{u}^{'} = \mathbf{u} - \mathbf{Lv}. \tag{12}$$

The cumulative quadratic error is showed in the math expression bellow:

$$\mathbf{S} = \mathbf{e^T e} = (\mathbf{u} - \mathbf{Lv})^{\mathbf{T}}(\mathbf{u} - \mathbf{Lv}), \tag{13}$$

and minimizing S respect to v, we will have:

$$\mathbf{v} = (\mathbf{L^T L})^{-1}\mathbf{L^T d}, \tag{14}$$

with $(L^T L)^{-1} L^T$ as a inverse matrix of L. However, the inverse matrix of L is not possible to obtain in pracitce. Generally, the fourier trasnform is applied, changing the domain from time to frequency, leading to a easier situation. Finally it is possible to estimate the inverse radon transform and apply it to the seismic data.

The Seismic Processing Workflow

In this work, the processing started importing the SEG-Y field files into the Seisspace for geometry assembly. The next step consists of editing and mute noisy traces and defective stations in land data. Next, first breaks picking is performed to be used in statics corrections, in order to eliminate the effects of the weathering layer and irregular topography. The next step is the ground-roll filtering, using the available tools in Seisspace/Promax 2D. To work with deconvolution, the data were, at first, exported to Seismic Unix, where they were organized in the CDP gathers. We applied MMO (Multiple velocity moveout) correction. We applied multi-channel predictive deconvolution and its results were re-imported into the Seisspace in SEG-Y format, where amplitude gains and spherical divergence correction and NMO correction were applied to finish the work with the stacking. In orther hand, to work with Radon Parabolic Transform, we applied NMO correction in the data organized in CDP domain in oder to separate the primary and multiple reflecions by their differents move-outs. The data were then passed to the Radon domain where the primary reflections showed a negative move-out $-q$ and the multiples reflections and reverberations showed a positiv move-out $+q$. After selecting the primary reflection region by applying a simple mute, we turn back to time domain through Radon Parabolic Inverse Transform, generating a filtered CDP as a output. The flowchart used is shown in Figure 1. At the end, we applied MMO correcion in these CDP gathers filtered by both methods in order to compare and visualizing their effect on multiples.

Results

The steps of the processing illustrated in Figure 1 were aimed at increasing the signal-to-noise ratio and grond-roll filtering. The pulse deconvolution and spectral balancing included in the filtering step promoted an increase in the frequency content of the data and a better definition of the reflections. A CDP was chosen to perform multichannel predictive deconvolution and Radon tests. In CDP 2867 illustrated in Figure 2a, a strong reflection in time 0.6s is observed and the associated multiple is found in time 1.2s. The MMO correction was applied with the velocity of 2200 m / s to horizontalise the primary and the multiple reflection (See Figure 2b). The predictive deconvolution was then applied, with 5 channels, from which the result shown in Figure 2c was obtained. It is well known that this method greatly attenuated the multiple. For the application of deconvolution in all CDPs, it was necessary to map the periods of the multiple ones in every section. It was also observed that the multiple reflections did not have exactly double the period in all the CDPs, as it occurs in marine data which do not present the problems related to irregular surface (different elevations between the points of fire and receivers) and weathering mantle. On the other hand, Radon filtering does not assume periodicity in the seismic data, witch is a strong point in this method. We applied NMO correction and then the Direct Radon transform were calculated. As we expected, in the $\tau - q$ domain, primary and multiples reflections were separated. In the Seisspace, supergathers were calculated to improve the noise and signal ratio and to avoid the aliasing on $\tau - p$ domain. We picked the region with more multiples than reflections

and erased from the transformed data before the inverse Radon to give it back to time domain. The output of this process were a CDP filtered with less interference from reverberations and multiples. Figure 3 shows the CDP with parcial NMO correction (parcial velocity) and its $\tau - q$ domain. We can notice the energy of primary reflections concentrated on the left side of its $\tau - q$ spectrum, as indicated by the arrows.

Despite the low signal-to-noise ratio, good results of these techniques were observed in the data analyzed in this study. Thus, for evaluation of the method, MMO correction was applied to all CDPs and then the stacked section was generated where only the primary and multiple reflections would be present, as shown in Figure 6a. After applying the deconvolution, the same procedure was repeated in the filtered data generating another stacked section, shown in Figure 6b. We repeated the same procedure and after Radon Filtering, we generated another stacked section, shown in Figure 6c. We can see that stacked section filtered from Radon shows more improvements in data quality than the deconvolved one. This is another expected result because coehrent noise generally has different move-out than reflections, and deconvolution depends on the periodicity of primary and multiple reflections. Although the attenuation was satisfactory at the end of the stacked section, where the multiple reflections had a larger amplitude, and in the beginning, with a weaker amplitude, the attenuation was less efficient in the central region, due to the non-periodicity of these events. It is clear that both methods employed generated good results, greatly attenuating the multiple reflection, as indicated by the arrows in both figures.

In addition, there was attenuation of reverberations associated to the multiple internal ones, which give the impression of lodging in the section. In Figure 4a, the CDP 2867 semblances are shown before and after the multichannel predictive deconvolution. In the original semblance (Figure 4a) we see the coherence related to the primary reflection at 0.6s time with 2200 m / s and another coherence close to 1.2s at the same speed. There are also several noises, which are not the object of this study. In Figure 5a and Figure 5b present two semblances calculated before and after Radon filtering. We can see cleary the difference between both velocity spectrums. In the semblance after filtering, it is observed that the energy related to the multiple reflection has been greatly reduced, besides the energy of the primary reflection has been emphasized. The results obtained in this work are still preliminary. It is intended to apply the multichannel predictive deconvolution in common offset families and improve the Radon filtering process to obtain better results and also combine both methods in a same workflow.

Conclusions

Finally, both methods, multichannel predictive deconvolution and Parabolic Radon Transform, could present satisfactory results in land seismic data, specifically in this case of Solimoes Basin, whose multiple events are associated to magmatic spills. The problems with elevation and thickness of the weathering layer with low signal-to-noise ratio common in land data can be bypassed in order to guarantee the effectiveness of the multi-channel predictive deconvolution method. Therefore, it is proposed to apply other methods of filtering for ground-roll attenuation different from conventional ones, such as the Singular Value Decomposition (SVD) method and the FDR (radial directional filtering) method in later works, Multichannel predictive deconvolution. The choice of the number of channels interferes greatly in the result obtained, since, at the beginning of this work, deconvolution results were analyzed with 5 channels and 10 channels, and with 10 channels the estimated filter acted quite strictly, also eliminating the primary reflections , And with 5 channels the estimated filter attenuated the multiple events better, improving the temporal resolution of the primaries. It was also observed that the input data of the deconvolution must be free of traces with null amplitude, since they are used in the estimation of the multichannel filter. Likewise, Parabolic Radon filtering depends on how accuratelly primary and multiple reflections can be separated by different move-outs. Data quality also interferes in this filtergin. It is noteworthy that the results obtained are still preliminary and other tests will be carried out with this methodology as well as other predictive deconvolution techniques. It is intended to follow the flowchart of processing, performing a new analysis of speeds, stacking and migration to obtain better results.

Acknowledgments

The authors thank the CPGG/UFBA/INCT-GP, for their support in developing this work. Marcelo thanks the CNPQ for the financial support.

References

Porsani M. J., Barros, A. Z. N. e Fernandes, R. A. R. 1997. Deconvolução de múltiplas com filtros Wiener Levinson multicanais. Anais do 5º Congresso Brasileiro de Geofísica.

da Silva, M. G. (2004) Processamento de dados sísmicos da bacia do Tacutu, Dissertação de Mestrado, Universidade Federal da Bahia.

Silmara L. R. Oliveira, Rosângela C. Maciel, Michelângelo G. da Silva e Porsani, M. J. (2014) Attenuation of short-period multiples in seismic data processing of the jequitinhonha Basin Brazil, Revista Brasileira de Geofísica, 32(3):395-403.

Eiras, J. F. (1989) Tectônica, sedimentação e sistemas petrolíferos da bacia do solimões, estado do amazonas, TAHA, M. Searching for oil and gas in the land of giants: the search magazine. Edição especial sobre Brasil. Argentina: Schlumbeger.

Yilmaz, O. (2001) Seismic data analysis: processing, inversion, and interpretation of seismic data, Investigations in Geophysics, Society of Exploration Geophysicists, 2º edic., ISBN, 978-1-56080-094-1.

Hampson, D. (1986) Numeric implementation of wave-equation migration velocity analysis operators, Journal of the canadian society of exploration geophysics, 22(1):44 to 55.

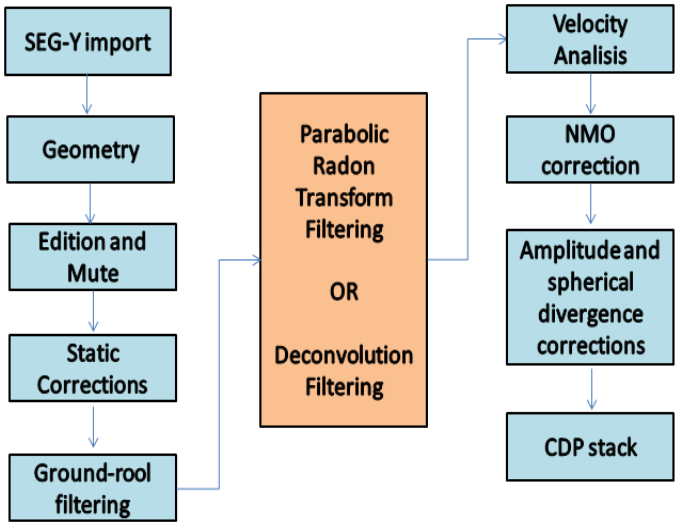

Figure 1: Workflow for seismic data processing.

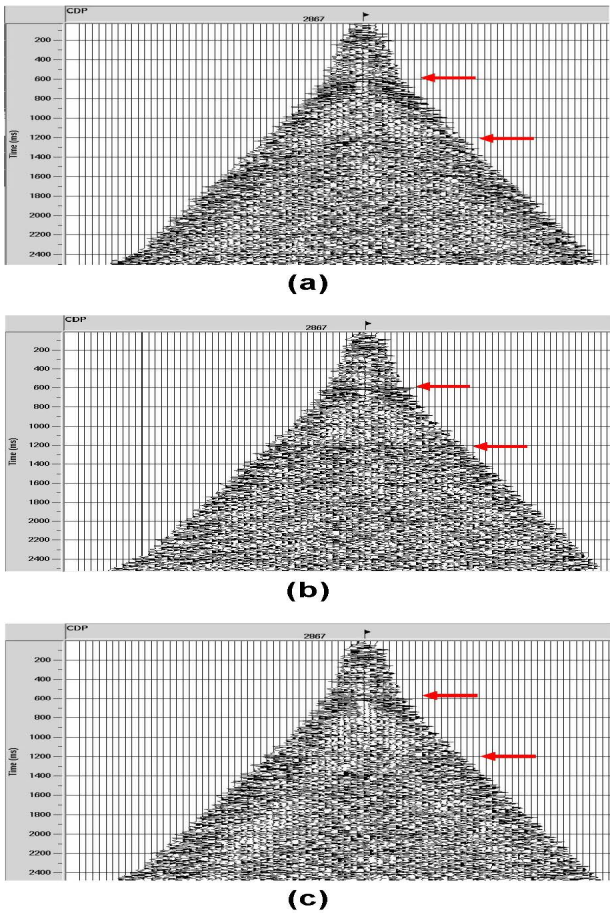

Figure 2: Display do Seisspace showing normal CDP (a), after MMO correction (b) and after MMO correction and deconvolution (c). Those arrows indicate primary reflections and multiples respectivelly.

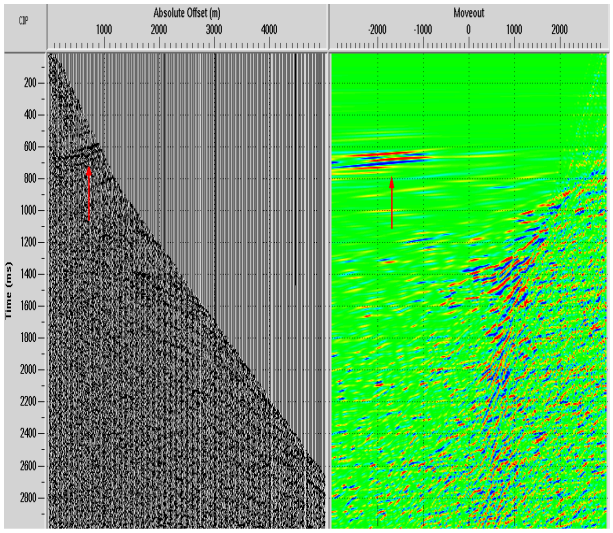

Figure 3: Display of Seisspace showing the CDP after NMO correction and its Radon spectrum. The arrows indicate the primary reflections.

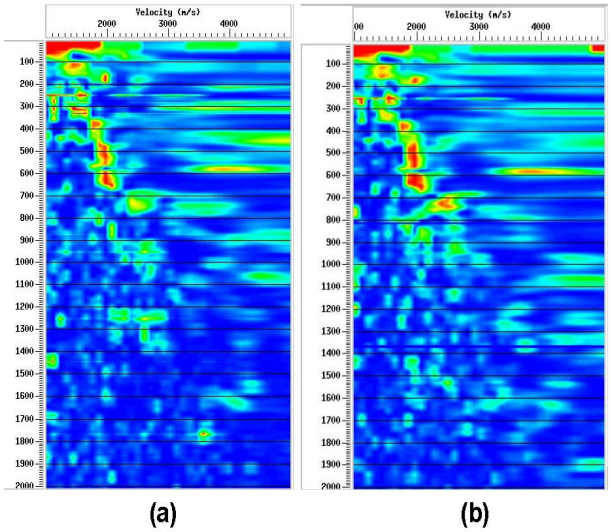

Figure 4: Display of Seisspace showing the Semblance spectrum for the CDP 2867 before (a) and after deconvolution (b). Note that deconvolution also enhanced the primary refleciton after attenuated the multiple reflection (1.2s a 1.3s).

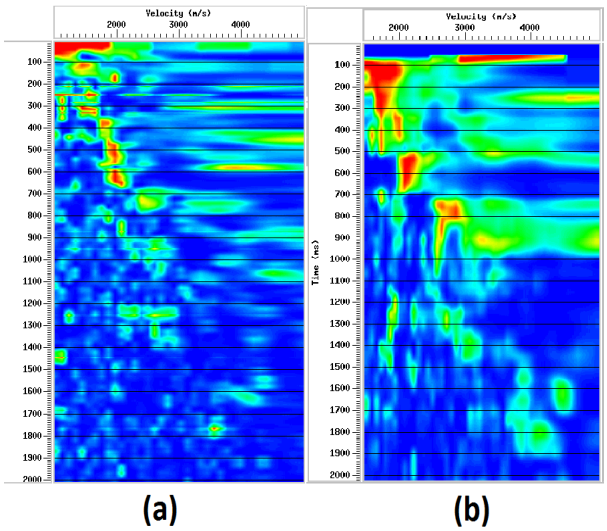

Figure 5: Display of Seisspace showing the Semblance spectrum for the CDP 2867 before (a) and after Radon Filtering (b). Despite the good results we achieved here, this spectrum is not as good as the output of deconvolution.

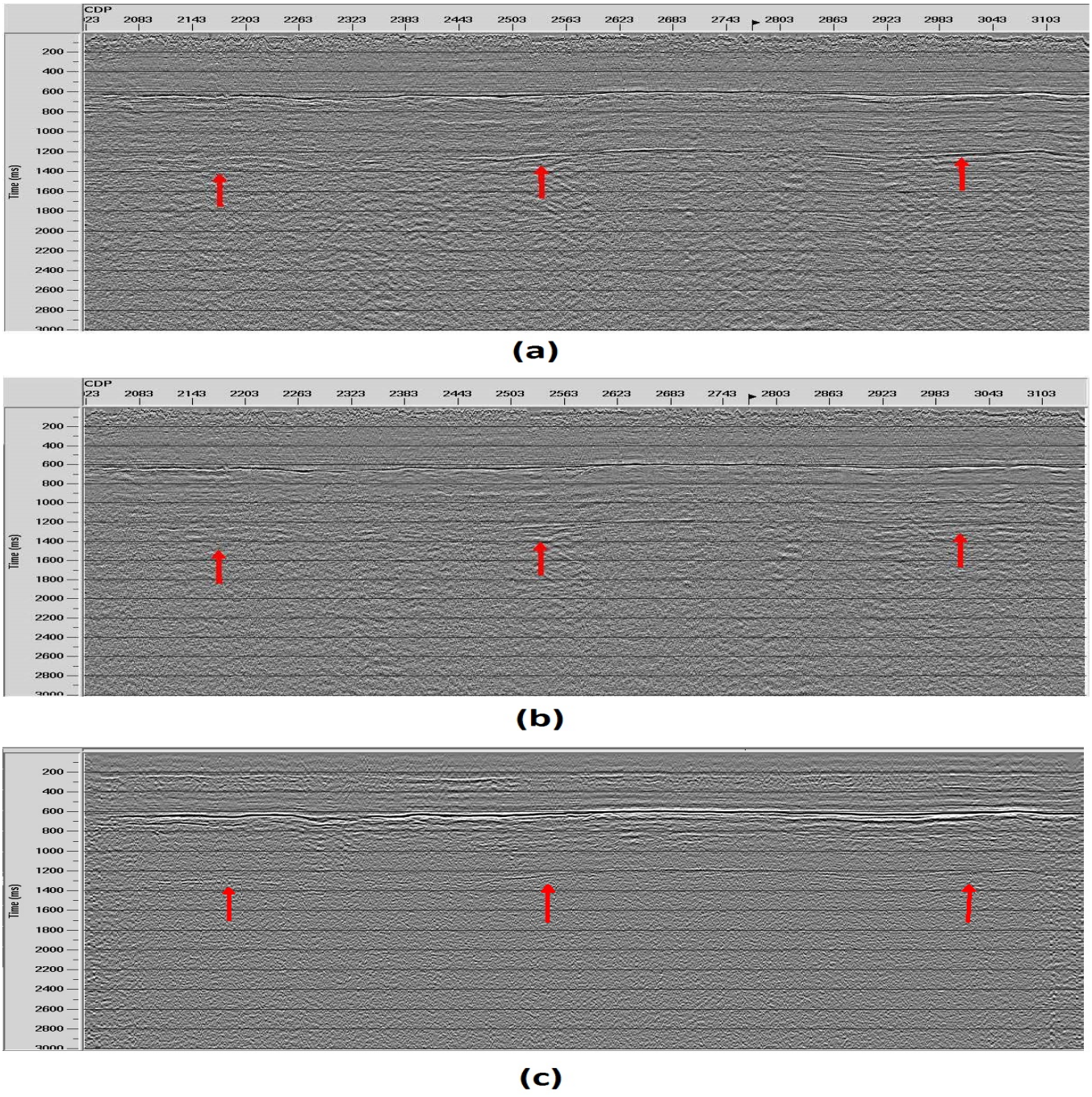

Figure 6: Display of Seisspace showing three stacked sections with brute MMO correction before filtering (a), after deconvolution and (c) after Radon filtering. Those arrows indicate the multiple reflection before filtering (a), and after filtering in (b) and (c). Preliminary results.